# Shiver me titin! Elucidating titin's role in shivering thermogenesis

Kari R. Taylor-Burt, Jenna Monroy, Cinnamon Pace, Stan Lindstedt, Kiisa C. Nishikawa

Short title: Titin mutation affects tremor frequency

Kewords: titin, shivering, thermoregulation, *mdm*, mouse

# Summary

Shivering frequency scales predictably with body mass and is ten times higher in a mouse than a moose. The link between shivering frequency and body mass may lie in the tuning of muscle elastic properties. Titin functions as a muscle "spring," so shivering frequency may be linked to titin's structure. The muscular dystrophy with myositis (*mdm*) mouse is characterized by a deletion in titin's N2A region. Mice that are homozygous for the *mdm* mutation have a lower body mass, stiffer gait, and reduced lifespan compared to their wildtype and heterozygous siblings. We characterized thermoregulation in these mice by measuring metabolic rate and tremor frequency during shivering. Mutants were heterothermic at ambient temperatures of 20-37°C while wildtypes and heterozygotes were homeothermic. Metabolic rate increased at smaller temperature differentials (i.e., the difference between body and ambient temperatures) in mutants than in non-mutants. The difference between observed tremor frequencies and shivering frequencies predicted by body mass was significantly larger for mutant mice than for wildtypes or heterozygotes, even after accounting for differences in body temperature. Together, the heterothermy in mutants, the increase in metabolic rate at low temperature differentials, and decreased tremor frequency demonstrate the thermoregulatory challenges faced by mice with the *mdm* mutation. Oscillatory frequency is proportional to the square root of stiffness, and we observed that mutants had lower active muscle stiffness *in vitro*. The lower tremor frequencies in mutants are consistent with reduced active muscle stiffness and suggest that titin affects the tuning of shivering frequency.

# Introduction

The natural resonating frequency of an oscillatory movement, such as tremor during shivering thermogenesis, depends on the properties of the material driving it. In the case of shivering, neural input (Stuart et al., 1966; Hohtola, 2004), animal size (Spaan and Klussmann, 1970; Günther et al., 1983; Kleinebeckel et al., 1994), and the mechanics and orientation of the body's materials (Stuart et al., 1966) could impact the frequency of oscillation. Muscle stiffness likely plays a role in determining the frequency of oscillatory motion in animals, such as tremor during shivering (Stuart et al., 1966). Muscle stiffness is determined, in part, by the molecular spring titin. We expect that changes in titin's structure could impact whole animal movement by modulating muscle stiffness. In this study, we investigate the effect of a titin mutation on muscles stiffness and on tremor during shivering thermogenesis.

Shivering thermogenesis is ideal for studying the effect of muscle stiffness on the whole animal level because it is muscle-driven and can be associated with oscillatory tremor (Stuart et al., 1966; Hohtola, 2004). The frequency ($f$) of simple harmonic motion can be modeled as

$$f = \frac{1}{2\pi}\sqrt{\frac{k}{m}} \tag{1}$$

where $m$ is the mass moved by the spring and $k$ is the spring constant. If we replace the spring constant with muscle stiffness, we would expect the frequency of oscillatory movements in animals to increase with increasing muscle stiffness and decrease with increasing body mass.

Much work on oscillatory movement has shown that body size is often correlated with frequency (Heglund and Taylor, 1988, Young et al., 1992, Lindstedt and Schaeffer, 2002 and references therein, Hurlbert et al., 2008, Sato et al., 2010, Dickerson et al., 2012). The frequency of muscle activation during shivering thermogenesis also seems to be correlated with body mass (Spaan and Klussmann, 1970). Relatively little work has related the frequency of oscillatory movements to muscle properties (Curtin and Woledge, 1993a,b) or compared stiffness to the frequency of movement (Young et al., 1992; Farley et al., 1993; Nassar et al., 2001). We can investigate the contribution of titin-based muscle stiffness to organism movement by comparing the frequency of tremor during shivering for animals with differences in titin structure and function.

The muscular dystrophy with myositis (*mdm*) mouse is characterized by a 779 bp deletion in the N2A region of the titin gene (Müller-Seitz et al., 1993; Garvey et al., 2002). This mutation is thought to contribute to changes in titin's structure (Lopez et al., 2008). The *mdm* mutants have a stiffer gait, smaller body mass, and reduced lifespan (Garvey et al., 2002; Witt et al., 2004; Huebsch et al., 2005; Lopez et al., 2008). A whole-muscle study on the diaphragm reported substantial

differences in the force production capabilities and elastic properties of *mdm* mutant muscle compared to wildtype muscle; of particular interest, mutant muscle has higher passive stiffness than wildtype muscle (Lopez et al., 2008).

We do not know the full extent to which titin may modulate muscle stiffness. Titin is a giant protein that is known to contribute to passive tension (Linke and Granzier, 1998; Lindstedt et al., 2002; Huebsch et al., 2005; Lopez et al., 2008; Leonard and Herzog, 2010; Herzog et al., 2012). Historically, titin was considered to have a static contribution to muscle stiffness since this protein is too compliant to substantially contribute to active muscle stiffness. However, Nishikawa et al. (2012) and Herzog (2014) have suggested that titin's contribution to muscle stiffness may increase upon muscle activation by binding to the thin filament. Leonard and Herzog (2010) and Powers et al. (2014) have shown that titin-based stiffness increases during muscle activation.

Our study aimed to investigate the effect of the *mdm* mutation on tremor during shivering thermogenesis. We tested two hypotheses: (1) changes in titin's structure due to the *mdm* mutation will affect tremor frequency during shivering and (2) changes in the frequency of tremor during shivering will affect metabolic rate. Specifically, we expected changes in muscle stiffness in the *mdm* mutants to correlate with changes in tremor frequency during shivering.

# Results

## Body Mass

At 30-50 days old, wildtype and heterozygous mice were significantly larger than *mdm* mutant mice (n = 6 for each genotype, $p < 0.0001$). Body mass did not vary significantly ($p = 0.1682$) between wildtypes (18.2 g ± 1.0 g) and heterozygotes (19.8 g ± 0.2 g). However, both wildtypes ($p < 0.0001$) and heterozgyotes ($p < 0.0001$) were about three times larger than age-matched mutant mice (6.3 g ± 0.3 g).

## Body Temperature

Ambient temperature, genotype, and their interaction had a significant effect on body temperature ($p < 0.0001$). Body temperature in wildtype ($p = 0.149$) and heterozygous ($p = 0.142$) mice did not vary with ambient temperature (Fig. 1), and body temperatures for these two genotypes were not significantly different ($p = 0.985$), with an average body temperature of 36.5°C ± 0.2°C for wildtypes and 36.8°C ± 0.2°C for heterozygotes. In contrast, the body temperature ($T_b$) of the mutant mice decreased at lower ambient temperature ($T_a$) ($p < 0.0001$; $T_b = 20 + 0.48T_a$). The mutants had a relationship that was significantly different from wildtypes ($p < 0.0001$) and heterozygotes ($p < 0.0001$).

## Metabolic Rate

Because mutant body temperature varies with ambient temperature (Fig. 1), establishing a baseline metabolic rate was problematic. In studies of heterothermic mammals (e.g., Heldmaier and Ruf, 1992), comparisons are made using the relationship between metabolic rate and the differential between body and ambient temperatures (i.e., temperature differential), where slope is the conductance (Scholander et al., 1950). Fig. 2 shows the metabolic rates for the temperature differentials measured at 20-30°C for wildtype and heterozygous mice and 30-35°C for mutants (see Methods for detail). Within this temperature range, the metabolic rates of mutants are in the same range as the metabolic rates observed in wildtype and heterozygous mice at ambient temperatures 5-10°C lower (Fig. 2).

The interaction between the temperature differential and genotype was not significant ($p = 0.1866$), meaning that thermal conductance was not significantly different among genotypes, so this interaction was removed from the model. Both genotype ($p = 0.0025$) and the temperature differential ($p < 0.001$) had a significant effect on metabolic rate, with a conductance of 0.55 $mL\ O_2\ hr^{-1}g^{-1}\ °C^{-1}$, which was significantly different from zero ($p < 0.001$), and y-intercepts of

0.26 $mL\ O_2\ hr^{-1}\ g^{-1}$ for wildtypes ($R^2$ = 0.70), 0.58 $mL\ O_2\ hr^{-1}\ g^{-1}$ for heterozygotes ($R^2$ = 0.56), and 4.3 $mL\ O_2\ hr^{-1}\ g^{-1}$ for mutants ($R^2$ = 0.18). The y-intercept for mutants was significantly different from zero (p < 0.001) while y-intercepts for wildtypes (p = 0.737) and heterozgyotes (p = 0.474) were not. The relationship for mutants was significantly different from wildtypes (p < 0.001) and heterozygotes (p < 0.001) but the relationships for wildtypes and heterozygotes were not different (p = 0.499).

Wildtype and heterozygous mice are three times larger than mutant mice, so they have reduced surface area/volume ratios and should have a lower conductance, which may explain why the mutants must generate metabolic heat at reduced temperature differentials. To account for the body size dependence of conductance, we compared the *mdm* mutants to *Baiomys taylori*, the pygmy mouse, which has an adult body mass of 6.4 g ± 1.3 g (Hudson, 1965), similar to the mutant body mass (6.3 g ± 0.3 g). The relationship for *B. taylori* based on data from Hudson (1965) is described by the equation $\dot{V}_{O_2} = -1.76 + 0.67(T_b - T_a)$. The relationship for *B. taylori* was not significantly different than for wildtypes (p = 0.163) or heterozygotes (p = 0.077) but was different from the mutant relationship (p < 0.001).

The highest metabolic rate measured was 10.4 $mL\ O_2\ hr^{-1}\ g^{-1}$ for mutants, 11.1 $mL\ O_2\ hr^{-1}\ g^{-1}$ for wildtypes, and 11.7 $mL\ O_2\ hr^{-1}\ g^{-1}$ for heterozygotes (Fig. 2). Mutant metabolic rates dropped at greater temperature differentials (personal observation), so it is likely that this represents the summit metabolic rate (i.e. the highest metabolic rate that can be elicited by cold stress) for mutants, at least under this set of experimental conditions. Metabolic rates of wildtypes and heterozygotes increased with greater temperature differentials within the range of temperatures used in this study, so there is no indication of whether the coldest temperatures used (20°C) were sufficient to achieve summit metabolic rate in these mice. Bozinovic and Rosenmann (1989) reported the following relationship for rodents:

$$SMR = 28.3m^{-0.338} \tag{2}$$

where $SMR$ is summit metabolic rate ($mL\ O_2\ consumed\ hr^{-1}\ g^{-1}$) and $m$ is body mass ($g$). Using this equation, the predicted summit metabolic rate was 14.9 ± 0.2 $mL\ O_2\ hr^{-1}\ g^{-1}$ for mutants, 10.5 ± 0.2 $mL\ O_2\ hr^{-1}\ g^{-1}$ for wildtypes, and 10.4 ± 0.2 $mL\ O_2\ hr^{-1}\ g^{-1}$ for heterozygotes, where the error represents variation in body mass.

**Shivering Frequency**

Mutants exhibited lower tremor frequencies during shivering but also had lower body temperatures than their non-mutant siblings. The mean tremor frequency during shivering was 35 ± 2

Hz for wildtypes, 31 ± 1 Hz for heterozygotes, and 19 ± 2 Hz for mutants (Fig. 3A). Genotype had a significant effect ($p < 0.001$). Although shivering frequency was not significantly different between wildtypes and heterozygotes ($p > 0.05$), frequencies were significantly higher for wildtypes and heterozygotes than for mutants ($p < 0.05$). As was found during the measurement of metabolic rate, mutants were heterothermic and body temperature varied among the three genotypes during shivering ($p = 0.003$). At 12-20°C, the average body temperature was 37.3°C ± 0.6°C with a range of 36.0-38.9°C for wildtype mice and 37.3°C ± 0.3°C with a range of 36.3-38.5°C for heterozygous mice. Mutant mice had an average body temperature of 33.0°C ± 0.8°C with a range of 28.9-35.6°C at ambient temperatures of 20-27°C. While wildtype and heterozygous mice did not have significantly different body temperatures ($p = 0.9858$), the average body temperatures of mutants were significantly lower than those of wildtype ($p = 0.0138$) and heterozygous ($p = 0.0138$) mice. Mutant tremor frequencies were corrected for body temperature using the $Q_{10}$ for the rate of muscle force production in mice, which Stein et al. (1982) reported as 2.5. Using that value, the body temperature-corrected average tremor frequency for mutants was 28 Hz ± 4 Hz (Fig. 3B). After correcting for body temperature, there was no effect of genotype on tremor frequency ($p = 0.2249$).

Mutants were much smaller than wildtypes and heterozygotes, and we know that body mass is correlated with shivering frequency. Using the relationship reported by Spaan and Klussmann (1970) between body mass and shivering frequency (based on electromyography, EMG), we calculated expected frequencies. We predicted that on average, mutants should have tremor frequencies of about 51 Hz while wildtypes and heterozygotes should have shivering frequencies of 41-44 Hz. Our observation that mutants shivered at frequencies equal to or lower than the frequencies observed for their siblings is surprising. On average, the differences between expected and observed (E-O) frequencies for all three genotypes were positive, indicating that the observed values fell below the expected values (Fig. 4). Both the individual ($p < 0.001$) and genotype ($p < 0.0001$) effects on E-O values were significant. The E-O values for mutants were significantly greater than the E-O values for wildtype and heterozygous mice ($p < 0.05$), but E-O values for wildtype and heterozygous mice did not differ significantly ($p > 0.05$).

Predictions based on body mass alone were higher than the observed values for wildtype (root mean square error (RMSE) = 19% and Akaike Information Criterion (AIC) = 44; predicted values: 41-44 Hz, observed values: 35.4 ± 1.8 Hz) and heterozygous mice (RMSE = 24% and AIC = 47; predicted: 41-44 Hz, observed: 31.0 ± 0.8 Hz). However, the differences between predicted and observed frequencies were much higher for mutants (RMSE = 63% and AIC = 61; predicted: 50-51 Hz, observed: 19.2 ± 1.7 Hz), even when accounting for differences in body temperature

(RMSE = 47% and AIC = 57; corrected: 28.3 ± 3.7 Hz).

Stiffness was measured in fully activated muscle *in vitro* (Fig. 5). The average stiffness was 174 $Nm^{-1}$ ± 60 $Nm^{-1}$ for mutant muscle and 982 $Nm^{-1}$ ± 97 $Nm^{-1}$ for wildtype muscle, and these stiffnesses were significantly different ($U = 12$, p = 0.02857). Using these stiffnesses and average body masses, we calculated the predicted frequency using Eqn. 1. We predicted tremor frequencies very similar to the observed tremor frequencies for both wildtype (predicted: 35-36 Hz; RMSE = 11% and AIC = 38) and mutant mice (predicted: 24-25 Hz; RMSE = 30% and AIC = 48). Adding stiffness resulted in substantially improved (i.e., lower) RMSE and AIC values for both wildtypes and mutants, which indicates that muscle stiffness is a useful parameter in predicting tremor frequency.

# Discussion

We have documented altered thermoregulation and shivering in *mdm* mutants compared to wildtypes and heterozygotes. In particular, the mutants are heterothermic and increase their metabolic rates at lower temperature differentials than age-matched siblings and the size-matched pygmy mouse. The mutant mice shiver with a lower tremor frequency than expected and have a lower active stiffness. A model of body mass alone predicts a higher tremor frequency in mutants than their larger siblings, while a model that accounts for both lower body mass and lower active stiffness in mutants predicts a lower tremor frequency. Thus, one consequence of the *mdm* mutation is a decrease in tremor frequency, which is likely linked to decreased active muscle stiffness.

**Body Temperature and Metabolic Rate**

We observed heterothermy in mutant mice but not in wildtype or heterozygous mice. The change in body temperature in mutants could reflect a torpor-based thermoregulation strategy, which is common among small mammals (Hudson, 1965; Heldmaier and Ruf, 1992). This seems an unlikely explanation because prior to a drop in body temperature, these animals increased their metabolic rates in response to decreased ambient temperatures, an opposite response to entering torpor. The plausible alternative hypothesis is that body temperature decreases because the rate of heat loss exceeds the rate of heat production, which could be the result of reduced thermogenic capacity, greater rate of heat loss, or both.

Heat for thermoregulation is produced through muscle-driven shivering and brown adipose-driven non-shivering thermogenesis. We may expect a reduction in heat production through shivering thermogenesis in the mutants because the *mdm* mutation affects muscle. However, we cannot rule out the possibility of differences in nonshivering thermogenesis in brown adipose tissue (Lonc̆ar, 1991; Klaus et al., 1998; Hu et al., 2010). While distinguishing between the importance of muscle-driven shivering thermogenesis, brown adipose-based nonshivering thermogenesis, and heat produced through other metabolic pathways is difficult, it is clear that the mice are heterothermic because heat production is quickly surpassed by heat loss.

The metabolic rate of *mdm* mutants increased at much lower temperature differentials ($T_b - T_a$) than age-matched siblings and sized-matched *Baiomys taylori*. Thus, the rate of heat loss exceeded the rate of heat production more readily in mutants, resulting in a higher critical temperature (i.e., the lowest ambient temperature at which metabolic cost of thermoregulation is minimal). According to the Scholander equation (Scholander et al., 1950), mutants must have higher conductance than their non-mutants siblings and *B. taylori* (see methods for more detail), although we did not find significant differences between the slopes (i.e., conductance) of the relationships between tem-

perature differential and metabolic rate. The small size and resulting high surface area to volume ratio is expected to cause a higher conductance and narrower thermoneutral zone in mutants; however, size cannot account for differences between *mdm* mutants and *B. taylori*. The lower body mass and emaciated appearance of these animals suggest that conductance could be higher due to diminished levels of insulating white adipose tissue. The stress of heterothermy and the metabolic cost associated with high conductance may play a role in limiting the growth of these animals and decreasing their lifespan.

Our highest measured metabolic rate (10.4 $mL\ O_2\ hr^{-1}\ g^{-1}$) fell short of the predicted value (14.9 $mL\ O_2\ hr^{-1}\ g^{-1}$) for mutants, but observed values were similar to, if not higher than, predicted values for wildtype and heterozygous mice. Mutants are subject to the $Q_{10}$ effects of dropping body temperatures (Fig. 1), which coincide with increases in the temperature differential. As body temperature falls, so must the summit metabolic rate. Therefore, we expect that summit metabolic rate in mutants is limited by body temperature and that the calculated mutant conductance may, consequently, be an underestimate.

Reduced heat production or increased conductance could cause heterothermy in the *mdm* mutants. A reduction in shivering thermogenesis due to altered muscle function is a simple explanation. If thermogenesis is reduced due to low shivering frequencies, metabolic rate may be limited by $Q_{10}$ effects, which could in turn affect other types of thermogenesis. However, the mutants increased metabolic rate at lower temperature differentials than their siblings, indicating that they are also losing heat faster. Thus, the heterothermy in mutants is likely due to high conductance but could also be linked to lower heat production. More studies are needed to distinguish the contributions of lower thermogenesis and higher conductance to mutant heterothermy.

**Tremor Frequency**

Body mass, body temperature, and muscle stiffness should all be considered when measuring tremor frequency. We used Eqn. 6 to normalize for body temperature. We accounted for differences in body mass and muscle stiffness using two models. (1) First, we used a model for body mass alone (Eqn. 5) and found that the difference between expected and observed tremor frequencies was significantly larger for mutants than for wildtypes and heterozygotes. (2) Second, we measured active muscle stiffness and found that mutant muscle had lower active stiffness than wildtype muscle. A model that included both body mass and muscle stiffness (Eqn. 1) produced better predictions for tremor frequency for both wildtypes and mutants, with an especially large improvement in the predictions for mutants.

*Mass Only Model*

Spaan and Klussmann (1970) produced an allometric relationship between body mass and shiv-

ering frequency using animals with a wide range of body masses, from mice with an average body mass of 40 g to dogs with an average body mass over 11 kg. This relationship has since been shown to hold for larger animals (i.e., humans, Schneider and Brooke, 1979) as well as smaller animals (i.e., shrews, Kleinebeckel et al., 1994), the smallest of which have a body mass of 4-5 g, smaller than the *mdm* mutants. Fig. 6 includes our data, studies that reported shivering frequencies measured using EMG (i.e. the frequency of changes in electrical activity within the muscle; Spaan and Klussmann, 1970; Schneider and Brooke, 1979; Günther et al., 1983; Kleinebeckel et al., 1994), and studies that reported the frequency of tremor (i.e., the frequency of movement of the body or a part of the body; Schneider and Brooke, 1979; Hohtola and Stevens, 1986). All three genotypes had lower than expected shivering frequencies, likely due to differences in EMG and tremor frequencies. However, the difference between expected and observed values for mutants was significantly larger than for wildtypes and heterozygotes as we would expect the smaller mutants to have a higher tremor frequency rather than at a frequency similar to or lower than that for the larger wildtypes and heterozygotes. In fact, the 6.3 g mutants shivered at a frequency that we would expect for an animal of more than 100 g. Thus, this model based on body mass provided a poor prediction of shivering frequency for mutants.

Although we are making an intraspecific comparison, we cannot ignore the effect that body mass is known to have on shivering frequency in mammals (Spaan and Klussmann, 1970; Günther et al., 1983; Kleinebeckel et al., 1994), particularly because the *mdm* mutants are far outside the normal range of body mass in adult laboratory mice. Spaan and Klussmann (1970) reported that similarity in body mass, not relatedness of species, resulted in similar shivering frequencies. Furthermore, Kleinebeckel et al. (1994) measured shivering frequency for several species in the *Crocidurinae* and *Sorcinae* shrew subfamilies. They found there was substantial variation in shivering frequency within the subfamily *Crocidurinae*, with smaller species exhibiting shivering frequencies more similar to small *soricines* than to other *crocidurine* species. Our use of the interspecific allometric relationship is appropriate in this case because (1) all of the animals we studied fall within the range of body masses in which this relationship applies, (2) the *mdm* genotypes have significantly different body masses, and (3) body mass is a stronger predictor of shivering frequency than phylogeny.

The EMG frequency reflects muscle stimulation during shivering, but there is likely damping from viscoelastic structures and the mass of the body (Stuart et al., 1966). Thus, while they are related, we expect small differences between the EMG frequency and tremor frequency. In fact, our data support damping because the observed tremor frequency was lower than the EMG-based prediction for all three genotypes. However, the difference between expected and observed fre-

quencies for mutant mice was significantly larger than for the other *mdm* genotypes, suggesting that it was not damping alone that caused the reduced tremor frequency we observed in the mutants. Furthermore, we were able to model shivering as a simple harmonic oscillation and make very good predictions of shivering frequency based on body mass and active muscle stiffness.

*Mass and Stiffness Model*

We predicted tremor frequencies by using Eqn. 1 and *in vitro* measurements of active muscle stiffness. Our measurements show that mutants have a lower active muscle stiffness than wildtypes. By using a model that included stiffness, not just body mass, we were able to make better predictions for shivering frequency for both wildtypes and mutants. This suggests that muscle stiffness may play an important role in shivering thermogenesis. It may also indicate that the larger difference between expected and observed shivering frequencies for mutants could be accounted for by differences in active muscle stiffness.

The lower tremor frequency observed in *mdm* mutants could also be caused by slower contraction rates and/or lower passive stiffness. Although Lopez et al. (2008) found a higher slow:fast ratio for myosin heavy chain isoform in mutant muscle than in non-mutant control muscles, these authors reported that mutant muscle actually had a shorter time to peak force and a shorter half-relaxation time compared to non-mutant controls. Therefore, if tremor frequency were dependent on muscle contraction kinetics, we would expect that mutants would shiver at or above expected tremor frequencies, not below, as we observed.

Passive stiffness may also affect shivering frequency. Passive stiffness and passive tension are higher in mutant muscle than in wildtype muscle for whole muscle experiments (Lopez et al., 2008), although Witt et al. (2004) did not observe differences in passive tension in single muscle fibers. Higher passive stiffness could result from the presence of more collagen and/or from a shorter titin spring (Lopez et al., 2008). An increase in muscle stiffness should result in an increase in tremor frequency for *mdm* mutants, not a decrease in tremor frequency, as we observed.

Thus, titin may be implicated as simultaneously contributing to reduced active stiffness and increased passive stiffness in *mdm* mutants. Leonard and Herzog (2010) and Powers et al. (2014) observed that titin-based muscle stiffness increases upon activation. It is plausible that the mechanism by which titin increases active muscle stiffness is affected by the *mdm* mutation (Nishikawa et al., 2012; Herzog, 2014). Our observations of lower tremor frequency and reduced active stiffness in mutant muscle are consistent with the hypothesis that titin is an important modulator of active muscle stiffness.

## Conclusions

The combination of the higher metabolic cost of thermoregulation and the inability of mutants

to remain homeothermic suggests that the *mdm* mutation may be an ideal model to study the limitations of thermoregulation. Differences in shivering frequency cannot be explained by changes in contraction kinetics or by changes in passive muscle stiffness. Our results demonstrate that mutants shiver at lower frequencies than predicted which may be best explained by the lower active muscle stiffness that we observed *in vitro*. Titin may provide the tuning of shivering frequency through its role in setting active muscle stiffness.

# Materials and methods

## Mice

Breeding pairs of B6C3Fe *a-/a-mdm* mice (*Mus musculus*, Linnaeus) were purchased from the Jackson Laboratory (Bar Harbor, ME, USA) and used to establish a colony. The *mdm* mutation is recessive, so heterozygous mice were bred to obtain pups that had homozygous wildtype, heterozygous, and homozygous mutant genotypes. Heterozygous and wildtype mice were indistinguishable, so ear punches and tail snips were used for genotyping following the methods of Lopez et al. (2008). The mice were fed *ad libitum* and housed at 23-24°C with a 14:10 light:dark cycle. Mutants were housed in cages that rested partially on a heating pad to allow these animals to select a warmer environment. All animal procedures were approved by the Institutional Animal Care and Use Committee at Northern Arizona University.

Wildtype pups reach a body mass comparable to adult mutant body mass (i.e., approximately 6 g) within 2 weeks after birth, which is near the time when shivering thermogenesis is observed but before these animals are weaned and capable of independently thermoregulating for long periods (Chew and Spencer, 1967). Thus, size-matching the animals was not appropriate as differences in metabolic rate and shivering frequency between neonatal wildtype mice and adult mutant mice could reflect developmental rather than genotypic differences. We chose to instead measure metabolic rate and shivering frequency in age-matched mice.

Because of the short lifespan of mutants, their general fragility, and the need to use these animals in terminal experiments within a certain age-range, we used different animals for each set of experiments and could not collect all data from a given individual. Genotype of wildtypes and heterozygotes was often not known until after the animal was sacrificed, so controlling these sample sizes was difficult. Large changes in body temperature caused concern for animal welfare, so sample sizes for mutants at very low ambient temperatures were limited. As a result, the sample size varies from experiment to experiment and from data point to data point. Details about sample sizes are given in Table S1.

## Temperature Measurements

Body and ambient temperatures were measured using small T-type thermocouples (copper-constantan, Omega Engineering, Inc., Stamford, CT, USA). Mice were anesthetized using isoflurane USP (MWI Veterinary Supply, Boise, ID, USA), which was administered in vapor form using a Forane vaporizer (Ohio Medical Corporation, Gurnee, IL, USA). During anesthesia, the animal was placed on a heating pad and provided a continuous flow of anesthetic (1-2% isoflurane:oxygen mixture for wildtypes and heterozygotes; 0.5-1% for mutants) through a nose cone. While the mouse was under anesthesia, a thermocouple was inserted into the rectum (Good, 2005) and secured by attaching

the lead to the tail with cloth medical tape. The thermocouple was inserted 2 cm for wildtype and heterozygous mice (Good, 2005) but only 1 cm (Dirks et al., 2002) for the much smaller mutant mice; these depths were reported by others to provide accurate body temperature measurements while avoiding injury. A similar thermocouple was placed in the animal's chamber to measure ambient temperature. Body and ambient temperature were monitored using the HH127 TC Datalogger (Omega Engineering, Inc., Stamford, CT, USA) and were sampled at a rate of 1 sample / minute. Body temperatures displayed in Fig. 1 were taken after the ambient temperature was ramped from room temperature to test temperature over 20 minutes and held constant for at least five minutes.

**Metabolic Rate Measurements**

Metabolic rates were measured over a range of temperatures (20-37°C) for mice that were 29-60 days old (wildtypes: n = 8; heterozygotes: n = 7; mutants: n = 10) with 2-6 animals measured at each temperature. Each animal was anesthetized and a thermocouple was inserted rectally, as described above. All animals recovered for a minimum of 20 minutes before measurements were taken. Animals were placed in a small, air-tight chamber (4.7 cm X 10 cm X 7 cm). A pump (Model R2 Flow Control; Applied Electronics, Sunnyvale, CA, USA) applied positive pressure to ambient air to push it through the chamber at a minimum of 300 $mL\ min^{-1}$. The air passed through a copper coil prior to entering the chamber, and both the copper coil and the chamber were placed in a water bath in order to manipulate the chamber temperature. Air was scrubbed of water using a drierite column both before entering the chamber and after leaving the chamber before oxygen measurements. The animal was placed in the chamber and allowed to acclimate for a minimum of 20 minutes before any measurements were made. A Matheson Mass Flow Readout (Model 8102-1452-FM; Tokyo, Japan) recorded flow rate, and an FC-10 Oxygen Analyzer (Sable Systems; Las Vegas, NV, USA) measured oxygen levels. A NI USB-6009 data acquisition device relayed these data to a custom LabView program (see Fig. S1 for an example). Data were collected at 4 Hz. Metabolic rate was the average oxygen consumption over a minimum of 60 seconds that was measured when the animal was still and oxygen consumption showed little variability. Oxygen uptake was measured in this open flow system using the equation from Lighton (2008):

$$\dot{V}_{O_2} = \frac{\dot{V}_I * (F_{I_{O_2}} - F_{E_{O_2}})}{1 - (F_{I_{O_2}} * (1 - RQ))} \tag{3}$$

where $\dot{V}_I$ is the rate of air flow ($mL\ min^{-1}$), $F_{I_{O_2}}$ is the volume fractional concentration of oxygen entering the chamber (or ambient oxygen level), $F_{E_{O_2}}$ is the volume fractional concentration of air exiting the chamber, and $RQ$ is respiratory quotient, which is assumed to be 0.85. Note that a 10%

error in RQ would result in a 1.8% error in the measurement. Measurements were taken after the animal had been in the chamber at least 20 min which is a full 18 "washout" times, as the total volume of the system was calculated to be 329 $mL^3$. Mass-specific metabolic rate was calculated in units of $mL\ O_2\ hr^{-1}\ g^{-1}$.

Here we define thermal conductance as the overall heat transfer coefficient, which incorporates heat lost by radiation and convection as well as conduction. In the following equation where $\dot{V}_{O_2}$ is metabolic rate in $mLO_2\ g^{-1}$, $T_b$ is body temperature in $^\circ C$, and $T_a$ is ambient temperature in $^\circ C$,

$$\dot{V}_{O_2} = C(T_b - T_a) \tag{4}$$

conductance ($C$) has the units of $mLO_2\ g^{-1}\ ^\circ C^{-1}$ (Scholander et al., 1950). This equation, first used by Scholander et al. (1950), has been referred to as "Newton's law of cooling." In order to determine the conductance (i.e., rate of heat loss), we found the relationship between metabolic rate and the temperature differential between body and ambient temperature. We did not include measurements above the thermoneutral zone. We used the temperature range of 20-30°C for wildtype and heterozygous mice because 30°C can be considered the point of thermoneutrality (Hussein, 1991) or the center of thermoneutral zone (Gordon, 2004). Mutant mice did not maintain a constant body temperature (Fig. 1), so determining their thermoneutral zone was difficult. Metabolic rate seemed to reach a minimum at 34-35°C, but when ambient temperature dropped below 30°C, metabolic rates of the mutant mice tended to drop with decreasing ambient temperature (personal observation). Therefore, temperatures ranging from 30-35°C were used for the mutants.

**Shivering Frequency**

Six age-matched (30-50 day old) mice of each genotype were used for these experiments. In order to affix an accelerometer, the animals were anesthetized, as described above, and a chemical depilator (Nair: Church & Dwight Co., Princeton, NJ, USA) was used to remove a patch of fur on the dorsal side, posterior to the head. Animals were permitted to recover 2-24 hours prior to any other manipulation.

The accelerometer (model: ADXL213; Analog Devices, Norwood, MA, USA) was used to determine tremor frequency during shivering with a sampling frequency of 1000 Hz. A NI USB-6009 data acquisition device (National Instruments, Austin, TX, USA) provided a 5 V power source for the accelerometer and relayed the signal to a custom LabView (Version 10.0, National Instruments, Austin, TX, USA) data acquisition program. Fine wires (0.13 mm copper wire, California Fine Wire, Grove Beach, CA, USA) provided lightweight leads, and thicker wire (1.3 mm, tin-copper wire, Consolidated Electronic Wire & Cable, Franklin Park, IL, USA) served as a point of at-

tachment to the accelerometer. The accelerometer was wrapped in electrical tape to secure wire attachments. The total weight of the accelerometer, including wires and the electrical tape, was 0.45 g, which is < 8% of the body mass of the smallest animals used.

Mice were weighed just before the shivering trial. The accelerometer was glued to a small strip of the adhesive portion of a sterile bandage. Animals were anesthetized, as described above, and the bandage and accelerometer were applied to the region where fur had been removed. The accelerometer was oriented to measure acceleration along the long axis of the animal. The animals were permitted to recover at least 20 minutes prior to data collection.

Shivering trials took place in a hibernation chamber (Hotpack Corp., Philadelphia, PA, USA), which was capable of both heating and cooling. Animals were placed in a small glass cage inside the chamber. The thermoneutral zone for wildtype mice is 27-32°C (Gordon, 2004). Tremor measurements were made when the animal was below its thermoneutral zone and when shaking was visually confirmed. The chamber temperature was maintained in the range of 12-20°C for wildtype and heterozygous mice and 19-27°C for mutants in order to elicit shivering. The temperature range differed between genotypes because mutants tended to shiver at higher temperatures than non-mutant mice and because mutants were unable to maintain body temperature at lower chamber temperatures. We computed a linear model for shivering frequency with genotype and ambient temperatures as fixed effects in order to determine the effect of the wide range of ambient temperatures used to elicit shivering. Ambient temperature did not have a significant effect on shivering frequency for the range of temperatures used in this study ($p = 0.682$), so ambient temperature was not considered in further analysis of shivering frequency.

Body temperature was the average of the rectal temperatures recorded during tremor events. For each animal, 6-32 independent tremor events were analyzed. The accelerometer data for each tremor event were filtered using a bandpass filter (5 Hz-70 Hz). The lower limit (5 Hz) eliminated low frequency movement artifacts and the upper limit (70 Hz) eliminated high frequency noise above the highest expected tremor frequencies (about 50 Hz). The filtered data then underwent a fast Fourier transform (FFT) using a custom LabView program (Fig. S2). FFTs can be used to calculate the relative abundance of each frequency that occurs in the signal. The frequency with the largest relative amplitude (i.e., the most prevalent frequency) from each trial was included in the calculation of the average shivering frequency for a given animal.

The relationship between shivering frequency and body mass is well established empirically (Spaan and Klussmann, 1970; Günther et al., 1983; Kleinebeckel et al., 1994). Spaan and Klussmann

(1970) reported the relationship between shivering frequency and body mass in mammals to be:

$$log(f) = 1.85 - 0.18log(m) \quad (5)$$

where $f$ is the mean shivering frequency ($s^{-1}$) and $m$ is mean body mass ($g$). Despite age-matching the mice, the body masses of the mutant mice (6.3 g ± 0.3 g) were much lower than the body masses of wildtype (18.2 g ± 1.0 g) and heterozygous mice (19.8 g ± 0.2 g). Using Eq. 5, we were able to calculate a predicted tremor frequency for each genotype and, thereby, take into account the differences in body mass.

**Correcting for Body Temperature**

Like other rates and the frequencies of other movements, tremor frequencies depend on body temperature (Schaeffer et al., 1996). Mutant mice often had body temperatures below normal body temperatures for mice (i.e., 37°C; Gordon, 2004). To account for these temperature differences, shivering frequencies were normalized in order to estimate the frequencies that would be expected if the mutants had a body temperature of 37°C. Stein et al. (1982) reported that the rate of force production for mouse muscle was temperature-dependent with a $Q_{10}$ of 2.5; metabolic rate in mice has a $Q_{10}$ of 2.4 (Geiser, 2004). These values are very similar, so we opted to use the muscle-specific value. Thus, we calculated expected tremor frequencies at a body temperature of 37°C using a $Q_{10}$ of 2.5 and the equation,

$$f_{corrected} = f_{obs} * Q_{10}^{\frac{37-T_{obs}}{10}} \quad (6)$$

where $f_{corrected}$ is the tremor frequency expected if body temperature is 37°C, $f_{obs}$ is the observed tremor frequency, and $T_{obs}$ is the observed body temperature.

**Stiffness Measurements & Modeling**

Soleus muscles were extracted from anesthetized wildtype (n=4) and *mdm* mutant (n=3) mice. The distal end of the muscle was attached to an inflexible hook and the proximal end was attached to a dual servomotor force lever (Aurora Scientific, Inc., Series 300B, Aurora, ON Canada) that measured position and force. In load-clamp experiments, muscles are rapidly unloaded and the change in muscle length due to the change in load can be used to measure active muscle stiffness during unloading. A series of load-clamp experiments was used to estimate the active stiffness of wildtype and *mdm* soleus muscles at stimulus frequencies corresponding to the shivering frequency, following the methods of Lappin et al. (2006). For each muscle, data from 6-8 load clamp tests were collected to model the active stress-strain relationship during active unloading using the

equation for an exponential spring,

$$F = F_0(e^{(x/d)} - 1) \tag{7}$$

where $F$ is force, $F_0$ and $d$ are constants that control the shape of the curve, and $x$ is strain.

**Statistical Analysis**

Analysis of variance (ANOVA) and Tukey's Honestly Significant Difference tests were used to compare body mass among genotypes. Body temperatures and muscle stiffnesses showed unequal variances among genotypes, so the non-parametric Wilcoxon test and Steel-Dwass comparisons were used to compare body temperatures and the Mann-Whitney test was used to compare stiffnesses.

The relationship between body temperature and ambient temperature, as well as the relationship between metabolic rate and the temperature differential (body temperature - ambient temperature), were compared using an analysis of covariance (ANCOVA) with genotype as a main effect. The ANCOVA model for metabolic rate and temperature differential did not include the temperature differential-genotype interaction term because this term did not significantly improve the model.

Average tremor frequency for each genotype was determined, and expected tremor frequency at 37°C was calculated using Eqn. 5. The expected-observed frequencies (E-O) were compared using a nested ANOVA that accounted for within-individual and within-genotype variation.

To compare models for predicting tremor frequency (i.e., body mass alone given by Eqn. 5 vs. body mass and stiffness given by Eqn. 1), we calculated root mean square error (RMSE) and Akaike Information Criterion (AIC). RMSE is defined by:

$$RMSE = \sqrt{\frac{\sum_N (f_{expected} - f_{observed})^2}{\sum_N f_{expected}^2}} * 100\% \tag{8}$$

where $f_{expected}$ is the expected frequency and $f_{observed}$ is the observed frequency (Perreault et al., 2003). AIC values are given by:

$$AIC = 2p - 2ln(L) \tag{9}$$

where $p$ is the number of parameters. Here, $ln(L)$ is defined such that:

$$ln(L) = 0.5 * (-N * (ln(2\pi) + 1 - ln(N) + ln \sum_{i=1}^{N} x_i^2)) \quad (10)$$

where $x_i$ is the residual and $N$ is the number of residuals (Spiess and Neumeyer, 2010).

A p-value $< 0.05$ was considered to be significant. Values are reported as average ± s.e.m. Statistical analysis was performed using JMP (v. 9 or 11, SAS Institute, Inc., Cary, NC, USA) and RStudio (v. 0.97.310).

# List of symbols and abbreviations

| Symbol or Abbreviation | Meaning |
|---|---|
| AIC | Akaike Information Criterion |
| ANCOVA | analysis of covariance |
| ANOVA | analysis of variance |
| bp | base pairs |
| $C$ | conductance |
| EMG | electromyography |
| E-O | expected - observed |
| $F$ | force |
| $f$ | frequency |
| FFT | Fast Fourier Transform |
| $k$ | stiffness |
| $m$ | mass |
| *mdm* | muscular dystrophy with myositis |
| $N$ | number |
| N2A | region of titin between PEVK and tandem Ig domains |
| RMSE | root mean square error |
| s.e.m. | standard error |
| $SMR$ | summit metabolic rate |
| $T$ | temperature |
| $T_a$ | ambient temperature |
| $T_b$ | body temperature |
| $\dot{V}_{O_2}$ | metabolic rate |
| $x$ | displacement |
| $x_i$ | residual |

## Acknowledgements

The authors would like to acknowledge the contributions of Erik Dillingham and David Tessmer who wrote custom data collection and analysis programs for this work. They would also like to thank Dr. Theodore Uyeno and Daniel Kmack for their help in designing the accelerometer, Joseph Kamper and Shane Meehan for help with data collection and troubleshooting, Dr. Scott Nichols for giving advice and guidance for animal protocols, and Thomas Greene and Leslie Hempleman for providing animal care. Finally, they would like to thank Paul Schaeffer and Anthony Hessel for helpful feedback on the manuscript.

## Competing interests statement

The authors declare no competing interests.

## Author contributions

KRTB, KCN, and SL contributed to the conceptual development and experimental design of this work. KRTB collected data for the shivering frequency and metabolic rate experiments, analyzed data, and drafted the manuscript. JM collected and analyzed the stiffness measurement data. CM was responsible for genotyping the mice. SL helped to develop the protocols used for collecting the metabolic rate data. KCN contributed funding. All authors contributed to the interpretation and presentation of the data and edited the manuscript.

## Funding

This work was supported by NSF IOS-1025806.

# References


**Bozinovic, F. and Rosenmann, M.** (1989). Maximum metabolic rate of rodents: physiological and ecological consequences on distributional limits. *Funct. Ecol.* **3**, 173–181.

**Chew, R. M. and Spencer, E.** (1967). Development of metabolic response to cold in young mice of four species. *Comp. Biochem. Physiol.* **22**, 873–888.

**Curtin, N. A. and Woledge, R. C.** (1993a). Efficiency of energy conversion during sinusoidal movement of red muscle fibres from the Dogfish *Scyliorhinus canicula*. *J. Exp. Biol.* **185**, 195–206.

**Curtin, N. A. and Woledge, R. C.** (1993b). Efficiency of energy conversion during sinusoidal movement of white muscle fibres from the Dogfish *Scyliorhinus canicula*. *J. Exp. Biol.* **183**, 137–147.

**Dickerson, A. K., Mills, Z. G. and Hu, D. L.** (2012). Wet mammals shake at tuned frequencies to dry. *J. R. Soc. Interface* p. doi: 10.1098/rsif.2012.0429.

**Dirks, A., Fish, E. W., Kikusui, T., van der Gugten, J., Groenink, L., Olivier, B. and Miczek, K. A.** (2002). Effects of corticotropic-releasing hormone on distress vocalizations and locomotion in maternally separated mouse pups. *Pharmacol., Biochem. Behav.* **72**, 939–999.

**Farley, C. T., Glasheen, J. and McMahon, T. A.** (1993). Running springs: speed and animal size. *J. Exp. Biol.* **185**, 71–86.

**Garvey, S. M., Rajan, C., Lerner, A. P., Frankel, W. N. and Cox, G. A.** (2002). The muscular dystrophy with myositis (*mdm*) mouse mutation disrupts a skeletal muscle-specific domain of titin. *Genomics* **79**, 146–149.

**Geiser, F.** (2004). Metabolic rate and body temperature reduction during hibernation and daily torpor. *Annu. Rev. Physiol.* **66**, 239–274.

**Good, D. J.** (2005). Using obese mouse models in research: special considerations for IACUC members, animal care technicians, and researchers. *Lab Anim. (NY)* **34**, 30–37.

**Gordon, C.** (2004). Effect of cage bedding on temperature regulation and metabolism of group-housed female mice. *Comp. Med.* **54**, 63–68.

**Günther, H., Brunner, R. and Klu$\beta$mann, F. W.** (1983). Spectral analysis of tremorine and cold tremor electromyograms in animal species of different size. *Pflügers Arch* **399**, 180–185.

**Heglund, N. C. and Taylor, C. R.** (1988). Speed, stride frequency and the energy cost per stride: do they change with body size and gait? *J. Exp. Biol.* **138**, 301–318.

**Heldmaier, G. and Ruf, T.** (1992). Body temperature and metabolic rate during natural hypothermia in endotherms. *J. Comp. Physiol., B.* **162**, 696–706.

**Herzog, W.** (2014). Mechanisms of enhanced force production in lengthening (eccentric) muscle contractions. *J. Appl. Physiol.* **116**, 1407–1417.

**Herzog, W., Duvall, M. and Leonard, T. R.** (2012). Molecular mechanisms of muscle force regulation: a role for titin? *Exercise Sport Sci. Rev.* **40**, 50–57.

**Hohtola, E.** (2004). Shivering thermogenesis in birds and mammals. *Life in the cold: evolution, mechanisms, adaptations, and application. 12th International Hibernation Symposium.* pp. 241–252.

**Hohtola, E. and Stevens, E. D.** (1986). The relationship of muscle electrical activity, tremor and heat production to shivering thermogenesis in Japanese Quail. *J. Exp. Biol.* **125**, 119–135.

**Hu, H. H., Smith, D. L., Nayak, K. S., Goran, M. I. and Nagy, T. R.** (2010). Identification of brown adipose tissue in mice with fat-water IDEAL-MRI. *J. Magn. Reson. Imaging* **31**, 1195–1202.

**Hudson, J. W.** (1965). Temperature regulation and torpidity in the Pygmy Mouse, *Biomys taylori*. *Physiol. Zool.* **38**, 243–254.

**Huebsch, K. A., Kudryashova, E., Wooley, C. M., Sher, R. B., Seburn, K. L., Spencer, M. J. and Cox, G. A.** (2005). *Mdm* muscular dystrophy: interactions with calpain 3 and a novel functional role for titin's N2A domain. *Hum. Mol. Genet.* **14**, 2801–2811.

**Hurlbert, A. H., Ballantyne IV, F. and Powell, S.** (2008). Shaking a leg and hot to trot: the effects of body size and temperature on running speed in ants. *Ecol. Entomol.* **33**, 144–154.

**Hussein, H. K.** (1991). Effect of temperature and body size on the metabolic rate of the Egyptian House Mice *Mus musculus* and the Roof Rat *Rattus rattus*. *J. Islamic Acad. Sci.* **4**, 249–252.

**Klaus, S., Münzberg, H., Trüloff, C. and Heldmaier, G.** (1998). Physiology of transgenic mice with brown fat ablation: obesity is due to lowered body temperature. *Am. J. Physiol. Regul., Integr., Comp. Physiol.* **274**, R287–R293.

**Kleinebeckel, D., Nagel, A., Vogel, P. and Klussmann, F.-W.** (1994). The frequencies of grouped discharges during cold tremor in shrews: an electromyographic study. *Integrative and cellular aspects of autonomic functions: temperature and osmoregulation* pp. 305–311.

**Lappin, A., Monroy, J., Pilarski, J., Zepnewski, E., Pierotti, D. and Nishikawa, K.** (2006). Storage and recovery of elastic potential energy powers ballistic prey capture in toads. *J. Exp. Biol.* **209**, 2535–2553.

**Leonard, T. R. and Herzog, W.** (2010). Regulation of muscle force in the absence of actin-myosin-based cross-bridge interaction. *Am. J. Physiol.: Cell Physiol.* **299**, C14–C20.

**Lighton, J.** (2008). *Measuring Metabolic Rates: A Manual for Scientists*. Oxford University Press.

**Lindstedt, S. L., Reich, R. E., Keim, P. and LaStayo, P. C.** (2002). Do muscles function as adaptable locomotor springs? *J. Exp. Biol.* **205**, 2211–2216.

**Lindstedt, S. L. and Schaeffer, P. J.** (2002). Use of allometry in predicting anatomical and physiological parameters of mammals. *Lab. Anim.* **36**, 1–19.

**Linke, W. A. and Granzier, H.** (1998). A spring tale: new facts on titin elasticity. *Biophys. J.* **75**, 2613–2614.

**Loncăr, D.** (1991). Convertible adipose tissue in mice. *Cell & Tissue Res.* **266**, 149–161.

**Lopez, M. A., Pardo, P. S., Cox, G. A. and Boriek, A. M.** (2008). Early mechanical dysfunction of the diaphragm in the muscular dystrophy with myositis ($Ttn^{mdm}$) model. *Am. J .Physiol.: Cell Physiol.* **295**, C1092–C1102.

**Müller-Seitz, M., Kaupmann, K., Labeit, S. and Jockusch, H.** (1993). Chromosomal localization of the mouse titin gene and its relation to “muscular dystrophy with myositis" and nebulin genes on chromosome 2. *Genomics* **18**, 559–561.

**Nassar, P. N., Jackson, A. C. and Carrier, D. R.** (2001). Entraining the natural frequencies of running and breathing in guinea fowl (*Numida meleagris*). *J. Exp. Biol.* **204**, 1641–1651.

**Nishikawa, K. C., Monroy, J. A., Uyeno, T. E., Yeo, S., Pai, D. K. and Lindstedt, S. L.** (2012). Is titin a ‘winding filament’? A new twist on muscle contraction. *Proc. R. Soc. B.* **279**, 981–990.

**Perreault, E. J., Heckman, C. J. and Sandercock, T. G.** (2003). Hill muscle model errors during movement are greatest within the physiologically relevant range of motor unit firing rates. *J. Biomech.* **36**, 211–218.

**Powers, K., Schappacher-Tilp, G., Jinha, A., Leonard, T., Nishikawa, K. and Herzog, W.** (2014). Titin force is enhanced in actively stretched skeletal muscle. *J. Exp. Biol.* Doi:10.1242/jeb.105361.

**Sato, K., Shiomi, K., Watanabe, Y., Watanuki, Y., Takahashi, A. and Ponganis, P. J.** (2010). Scaling of swim speed and stroke frequency in geometrically similar penguins: they swim optimally to minimize cost of transport. *Proc. R. Soc. B.* **277**, 707–714.

**Schaeffer, P. J., Conley, K. E. and Lindstedt, S. L.** (1996). Structural correlates of speed and endurance in skeletal muscle: the rattlesnake tailshaker muscle. *J. Exp. Biol.* **199**, 351–358.

**Schneider, M. F. and Brooke, J. D.** (1979). Bimodal relationship of human tremor and shivering on introduction to cold exposure. *Aviat., Space Environ. Med.* **50**, 1016–1019.

**Scholander, P. F., Hock, R., Walters, V., Johnson, F. and Irving, L.** (1950). Heat regulation in some arctic and tropical mammals and birds. *Biol. Bull.* **99**, 237–258.

**Spaan, G. and Klussmann, F. W.** (1970). Die frequenz des kältezitterns bei tierarten verschiedener größe. *Pflügers Arch.* **320**, 318–333.

**Spiess, A. N. and Neumeyer, N.** (2010). An evaluation of $R^2$ as an inadequate measure for nonlinear models in pharmacological and biochemical research: a Monte Carlo approach. *BMC Pharmacol.* **10**, doi: 10.1186/1471–2210–10–6.

**Stein, R. B., Gordon, T. and Shriver, J.** (1982). Temperature dependence of mammalian muscle contractions and ATPase activities. *Biophys. J.* **40**, 97–107.

**Stuart, D., Ott, K., Ishikawa, K. and Eldred, E.** (1966). The rhythm of shivering: II. Passive proprioceptive contributions. *Am. J. Phys. Med* **45**, 75–90.

**Witt, C. C., Ono, Y., Puschmann, E., McNabb, M., Wu, Y., Gotthardt, M., Witt, S. H., Haak, M., Granzier, H. and Labeit, S.** (2004). Induction and myofibrillar targeting of CARP, and suppression of the Nkx2.5 pathway in the MDM mouse with impaired titin-based signaling. *J. Mol. Biol.* **336**, 145–154.

**Young, I. S., Warren, R. D. and Altringham, J. D.** (1992). Some properties of the mammalian locomotory and respiratory systems in relation to body mass. *J. Exp. Biol.* **164**, 283–294.

Table S1. Samples Sizes by Experiment.
Note: $T_a$ are in °C and all measurements were taken within ±1°C of given temperature.

| Genotype | Shivering | Metabolic Rate and $T_b$ Measurement | | | | | | | | | | | |
|---|---|---|---|---|---|---|---|---|---|---|---|---|---|
| | $T_a$: | 20 | 24 | 26 | 28 | 30 | 31 | 32 | 33 | 34 | 35 | 36 | 37 |
| Wildtype | 6 | 3 | 3 | 3 | 3 | 3 | – | 3 | – | 4 | – | – | – |
| Heterozygous | 6 | 3 | 4 | 3 | 4 | 4 | – | 6 | – | 4 | – | – | – |
| Mutant | 6 | 2 | – | 3 | 3 | 4 | 3 | 4 | 3 | 3 | 4 | 3 | 3 |

Figure 1: **The relationship between body temperature and ambient temperature.** Resting body temperature for wildtype (n = 8), heterozygous (n = 7), and mutant mice (n = 10) as a function of ambient temperature. The dashed line serves as a reference line with a slope of one. The gray box shows the normal range of body temperatures for mice in typical housing conditions (i.e., ambient temperature of 23-24°C with bedding, Gordon, 2004). Points represent averages for measurements from 2-6 animals. Error bars represent standard error.

Figure 2: **Metabolic rate measurements for the *mdm* genotypes.** Mass-specific metabolic rate vs. the difference between body temperature and ambient temperature for the three *mdm* genotypes (wildtype: N = 8 animals, n = 15 total observations; heterozygote: N = 6, n = 18; mutant: N = 8, n = 20) and *B. taylori*, the pygmy mouse (Hudson, 1965). Temperatures used were within the range of temperatures over which metabolic rate increased with decreasing ambient temperature (i.e., metabolic rate doesn't decrease with decreasing temperature, nor were the measurements above the thermoneutral point). Metabolic rates shown here were measured at ambient temperatures between 20-30°C for wildtypes, heterozygotes, and *B. taylori* and between 30-35°C for mutants.

Figure 3: **Observed tremor frequency vs. body mass.** Tremor frequency during shivering for wildtype (n = 6), heterozygous (n = 6), and mutant (n = 6) mice. Boxplots represent individuals. The solid line gives the predicted frequency for a given body mass (Eqn. 5, Spaan and Klussmann, 1970). **(A)** The observed values of tremor frequency for all three genotypes. **(B)** Temperature-corrected tremor frequencies for mutants. Mutant body temperatures were lower than 37°C, so mutant tremor frequencies were corrected using a $Q_{10}$ of 2.5 and Eqn. 6 (see text).

Figure 4: **Comparing shivering frequencies across genotypes.** Average temperature-corrected tremor frequency was found for each genotype (n = 6 for each genotype). Expected shivering frequencies were found using Eqn. 5 (shown as solid line in Fig. 3). The average tremor frequency for mutants was calculated using the frequencies corrected for body temperature (Fig. 3B). The expected-observed (E-O) values for mutants were significantly greater than in wildtypes and heterozygotes ($p < 0.05$), but E-O values for wildtypes and heterozygotes did not differ significantly ($p > 0.05$). Error bars represent standard error.

Figure 5: **Active stiffness measurement.** Average wildtype (n=4) and mutant (n=3) stiffness under maximum stimulation. Error bars represent standard error.

Figure 6: **Allometric relationship between body mass and shivering frequency.** The line is the relationship reported by Spaan and Klussmann (1970) (Eqn. 5). The colored symbols represent the data from the current study, and error bars represent standard error. Black circles are data from other studies. Filled circles represent shivering frequencies measured using electromyography. The open circles represent the frequency of tremor during shivering. Error bars represent standard deviation or range, whichever was reported. The dashed lines show that the average tremor frequency for the *mdm* mutants (28 Hz ± 4 Hz) is a frequency we would expect to observe for an animal of > 100 g. This is surprising considering that the mutants are only 6-8 g. The numbers indicate different shrew species: 1, 3, 4 are in the Sorcinae subfamily (*Sorex minutes, Sorex coronets, Neomys fodiens*, respectively) and 2, 5, 6 are in the Crocidurinae subfamily (*Crocidura russula, Suncus murinus, Crocidura olivieri*, respectively). **Sources for Individual Data Points.** Shrews: Kleinebeckel et al., 1994; Mouse, rat, rabbit: Günther et al., 1983; Japanese quail: Hohtola and Stevens, 1986; human (both EMG and tremor frequencies): Schneider and Brooke, 1979 and references therein; cat and dog: Spaan and Klussmann, 1970.



Figure S1: **Representative oxygen and flow measurement.** In this example, the animal was placed in the chamber at 100 s and removed at 2000 s, at which times the chamber was opened and flow dropped. When the animal was in the chamber, the oxygen level dropped due to the animal's oxygen consumption. Measurements were taken when the animal was resting and after adjusting to the new environment for a minimum of 20 minutes; the data that fit these parameters are indicated by the gray box. Oxygen levels were calibrated using ambient oxygen levels (20.95%) and a calibration gas with a known level of oxygen. Combining oxygen levels and flow allowed us to determine oxygen consumption per unit time.

Figure S2: **Measurement of tremor frequency during shivering. (A)** These representative accelerometer data show one bout of shivering from an *mdm* mutant. **(B)** A fast fourier transform was used to find the most prevalent tremor frequency in each bout of shivering. In this example, the most prevalent frequency was about 12 Hz.

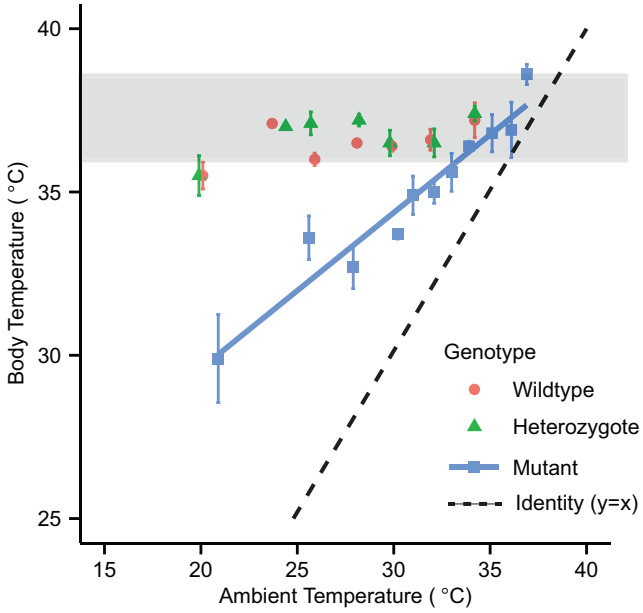


Figure 1:

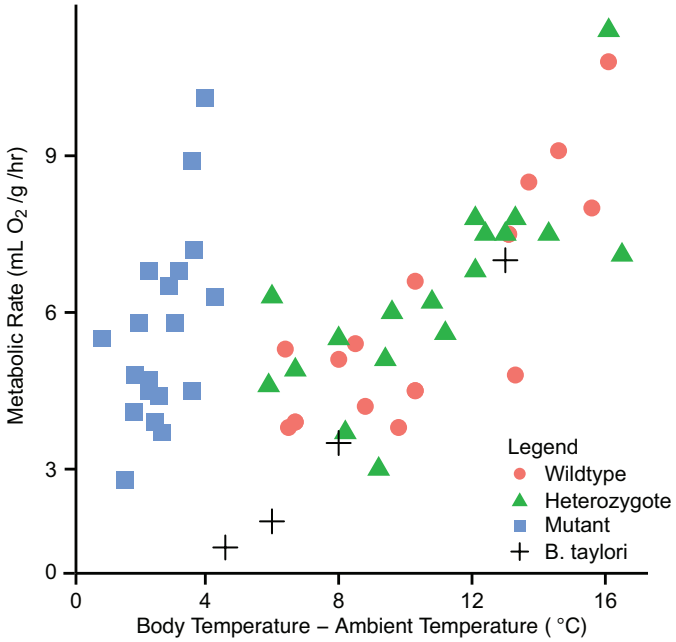


Figure 2:

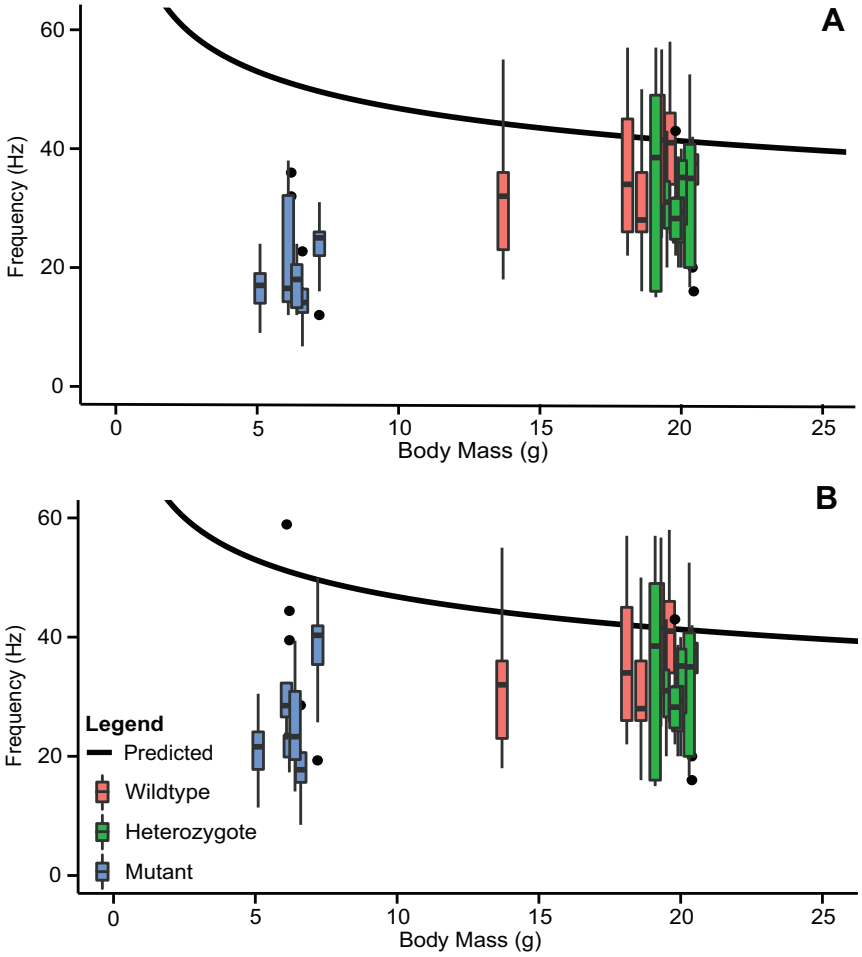


Figure 3:

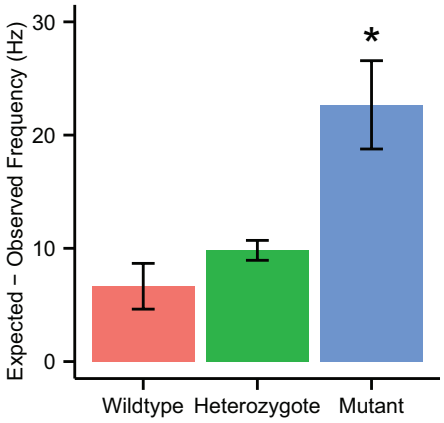


Figure 4:

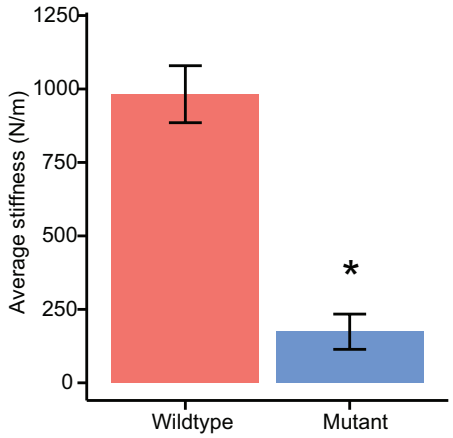


Figure 5:

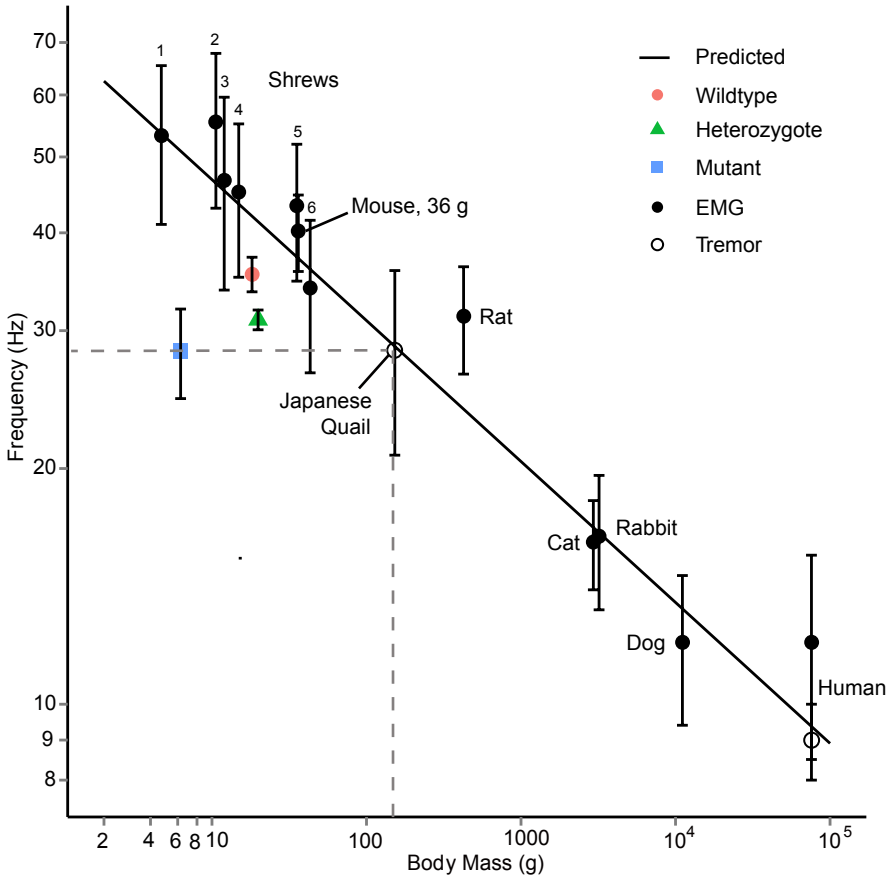


Figure 6:

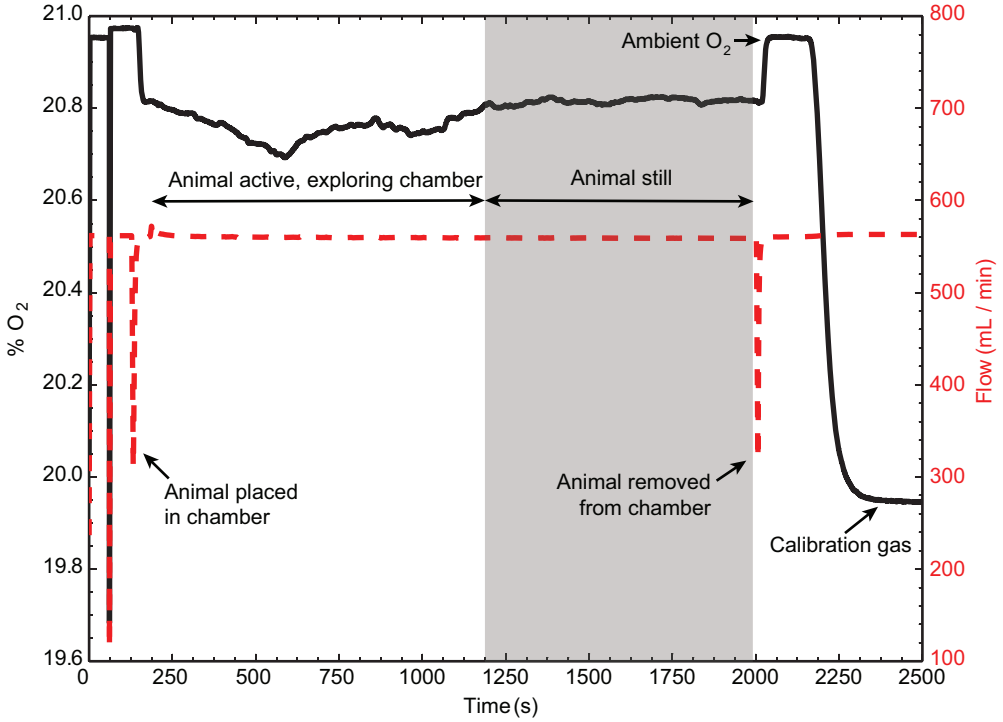


Figure S1:

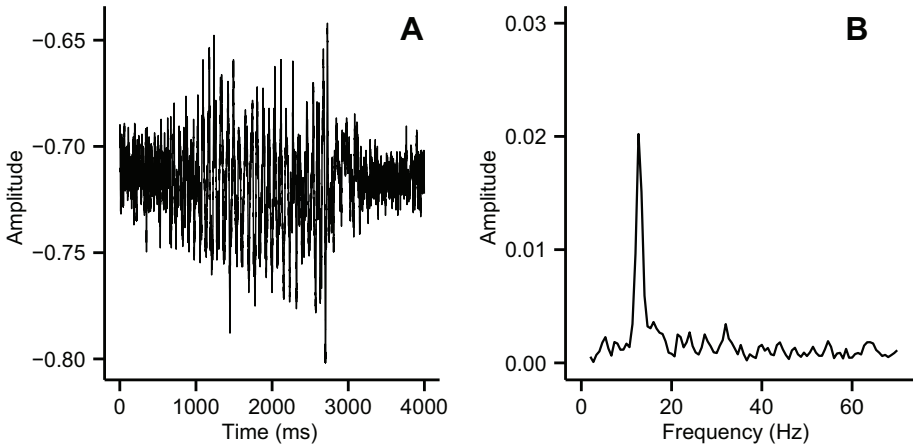


Figure S2: